



A Journal of the Gesellschaft Deutscher Chemiker

Angewandte Chemie

GDCh

International Edition

www.angewandte.org

Accepted Article

Title: High-Fidelity End-Functionalization of Poly(ethylene glycol) Using Stable and Potent Carbamate Linkages

Authors: Shengyu Shi, Chenzhi Yao, Jie Cen, Lei Li, Guhuan Liu, Jinming Hu, and Shiyong Liu

This manuscript has been accepted after peer review and appears as an Accepted Article online prior to editing, proofing, and formal publication of the final Version of Record (VoR). This work is currently citable by using the Digital Object Identifier (DOI) given below. The VoR will be published online in Early View as soon as possible and may be different to this Accepted Article as a result of editing. Readers should obtain the VoR from the journal website shown below when it is published to ensure accuracy of information. The authors are responsible for the content of this Accepted Article.

To be cited as: *Angew. Chem. Int. Ed.* 10.1002/anie.202006687

Link to VoR: <https://doi.org/10.1002/anie.202006687>

High-Fidelity End-Functionalization of Poly(ethylene glycol) Using Stable and Potent Carbamate Linkages

Shengyu Shi, Chenzhi Yao,⁺ Jie Cen,⁺ Lei Li, Guhuan Liu, Jinming Hu, and Shiyong Liu*

Abstract: *It is an open “secret” that commercial PEG-amine is of unreliable quality, for which we ascribe to both flawed manufacturing protocols and storage stability issues. In addition, conventional PEG functionalization relies on esterification and etherification steps, suffering from incomplete conversion, harsh reaction condition, and functional group incompatibility. To solve these practical challenges, we propose an efficient strategy for PEG functionalization through carbamate linkages. By finely tuning terminal amine basicity, stable and high-fidelity PEG-amine with carbamate linkage was successfully obtained, as evidenced from the clean set of MALDI-TOF MS pattern. The “carbamate” strategy was further applied to the synthesis of high-fidelity multi-functionalized PEG with varying reactive groups. Compared to that with ester linkage, amphiphilic PEG-PS block copolymers bearing carbamate junction linkage exhibits preferential self-assembly tendency into vesicles. Moreover, nanoparticles of the latter demonstrate higher drug loading efficiency, encapsulation stability against enzymatic hydrolysis, and improved in vivo retention at the tumor region.*

Poly(ethylene glycol) (PEG) has been the most well-known synthetic polymer across both academics and industry, with applications ranging from pharmaceuticals, biomaterials, cosmetics, and analytical science.^[1] Due to its biologically inert and biocompatible nature, PEG has been covalently conjugated with proteins, peptides, oligonucleotides, drugs, and lipids to extend *in vivo* circulation lifetime and stability, optimize pharmacokinetics, and reduce systemic toxicity.^[2] Up to date, over 10 pegylated proteins and peptides have received FDA approval.^[3] In addition, amphiphilic block copolymers (BCPs) synthesized using PEG-based initiators have been increasingly utilized to self-assemble into drug delivery nanocarriers, exhibiting extended blood circulation lifetime and reduced uptake by the reticuloendothelial system (RES).^[4]

End-group functionalized PEG is closely relevant to its functional applications. Due to its superior reactivity, primary amine-functionalized PEG has been extensively utilized for conjugation reactions and polymerization initiators.^[5] For example, amphiphilic PEG-polypeptide BCPs are synthesized using PEG-NH₂ as initiator.^[6] However, when the project was started four years ago, we soon realized that commercial PEG-NH₂ materials from main reagent suppliers and PEG-specialized manufacturers, either domestic or abroad, are of poor quality. GPC analysis gave multimodal elution peaks, and MALDI-TOF MS analysis revealed the presence of impurities unassignable to the specified structure

(Figure S1).^[7] mPEG-NH₂ is typically manufactured by converting hydroxyl group into sulfonyl ester (mesylate or tosylate), followed by treating with an excess of ammonium.^[5a-c,8] As already revealed in the original work published when MALDI-TOF MS technique was not available,^[5] this protocol inevitably leads to the formation PEG dimers and branched trimers. Note that either hydrogenation reaction of mPEG-azide or Staudinger reaction with PPH₃ is associated with similar side reactions,^[9] which are implicated by stronger basicity/nucleophilicity of newly generated secondary amines (Figure S1b). Impurities from these side reactions are clearly evident from GPC shoulder peaks of mPEG-NH₂ purchased from Fluka, Laysan Bio, and Nanocs (Figure S1). Moreover, we also found that the quality of commercial PEG-NH₂ gradually worsen up even when stored at -20 °C in a glovebox, implying functional group incompatibility between EG repeating units and terminal amines.

In general, end-group functionalization of PEG has been conventionally conducted through esterification or etherification of hydroxyl moiety (Scheme 1a). Esterification reaction is a reversible process and complete conversion could be only obtained under extreme conditions (anhydrous, excess reactant, elevated temperature, and potent condensation reagent).^[5b,10] In addition to its intrinsic hydrolytic tendency, ester linkage is also incompatible with primary amine moieties due to possible amidation reactions.^[11] Etherification reaction of PEG involves the use of strong bases (e.g., NaH) and might lead to PEG chain scission.^[12] On the other hand, previous studies revealed that carbamate linkage possesses superior stability towards both hydrolysis and aminolysis, as compared to ester and ether linkages.^[2c,13]

To solve these practical challenges associated with the quality and storage stability issues of PEG-NH₂, we hypothesize that carbamate linkage might be utilized for the synthesis of PEG-NH₂, and further generalized for various PEG derivatives (Scheme 1a). We propose that the storage stability issue is due to amine basicity based on a series of PEG-amine derivatives with varying spacers (Scheme 1b). The successful synthesis of stable PEG derivatives with high-fidelity terminal functionality are evidenced from the clean set of MALDI-TOF MS patterns. Moreover, nanostructures self-assembled from amphiphilic BCPs with carbamate junction linkage possess improved drug loading efficiency, encapsulation stability, and enhanced *in vivo* retention at the tumor region, as compared to that of BCPs with ester junction linkage (Scheme 1c).^[14]

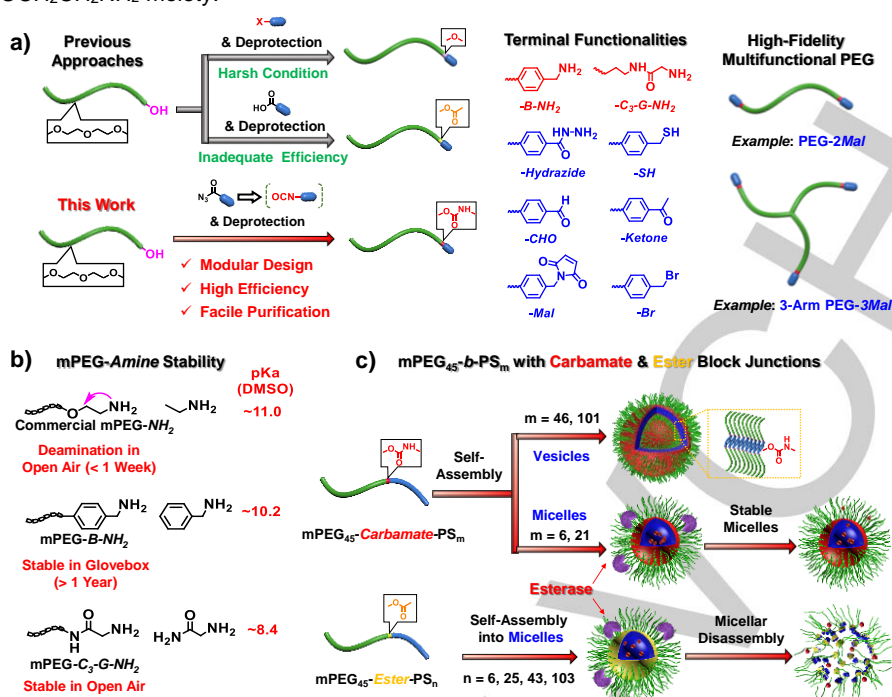
When two commercial mPEG₄₅-NH₂ samples (Laysan Bio and Nanocs) were stored for one week under open air at RT and 60 °C, GPC analysis revealed apparent shift to lower and higher MW side, respectively. These amine-mediated chain scission and coupling events are further implicated by air oxidation and amine carboxylation with CO₂ (Figure S1, c-d).^[15] Accordingly, MALDI-TOF MS analysis revealed increasing amount of deamination impurities (II, III) upon accelerated aging (Figure S1, e-g).^[12b,16] As these side reactions also occur when stored at -20 °C inside glovebox, we surmise that the instability mainly originates from amine basicity.^[17] Additionally, NH-O hydrogen bonding and superimposed O/N inductive effects might also contribute to

[*] S. Shi, Dr. C. Yao, J. Cen, L. Li, Dr. G. Liu, Dr. J. Hu, Prof. Dr. S. Liu
CAS Key Laboratory of Soft Matter Chemistry, Hefei National
Laboratory for Physical Sciences at the Microscale, Department of
Polymer Science and Engineering
University of Science and Technology of China
96 Jinzhai Road, Hefei, Anhui Province, 230026, China
E-mail: sliu@ustc.edu.cn

[†] Co-first authors

Supporting information and the ORCID identification number(s) for
the author(s) of this article can be found under:
<http://dx.doi.org/10.1002/anie.202006687>

instability of terminal $-OCH_2CH_2NH_2$ moiety.^[12b,16]



Scheme 1. a) Schematics of the synthesis of high-fidelity amine-functionalized PEG. The introduction of carbamate linkage via *in situ* generation of isocyanate from acyl azide moiety provides advantages over conventional ether and ester linkages in terms of linker stability, conjugation efficiency, and mildness of reaction conditions. The design was successfully applied to diverse terminal functionalities including hydrazide, thiol, aldehyde, ketone, maleimide, and bromine, and the fabrication of multi-functionalized PEG. This strategy could be further generalized to the post-functionalization of any hydroxyl and amine-containing precursors. b) The quality of commercial mPEG- NH_2 is less reliable due to side reactions (i.e., interchain coupling and branching) associated with manufacturing process and storage stability resulting from deamination reaction caused by amine basicity ($pK_a \sim 11$). Using the new strategy, the efficiency of end group functionalization is guaranteed and storage stability much improved for carbamate-incorporated mPEG- $B-NH_2$ and mPEG- C_3-G-NH_2 with decreasing amine basicities ($pK_a \sim 10.2$ and 8.4 , respectively). c) For amphiphilic block copolymers with different block junction linkages, mPEG₄₅-Carbamate-PS_m and mPEG₄₅-Ester-PS_n, the former prefers to self-assemble in aqueous media into vesicles, whereas the latter self-assembles into micellar nanoparticles at comparable PS chain lengths. Micellar nanocarriers of mPEG₄₅-Carbamate-PS_m possess excellent stability towards hydrolysis and enzymatic degradation, as compared to that of mPEG₄₅-Ester-PS_n.

Based on chemical intuition, we reasoned that benzyl amine-functionalized PEG with carbamate linker might possess improved stability due to decreased amine basicity ($pK_a \sim 10.2$ in DMSO) and decoupled N/O inductive effects in conventional PEG- NH_2 terminal (Figure 1a). Considering the moisture-sensitive and highly reactive nature of isocyanates, acyl azide derivative bearing benzyloxycarbonyl (Cbz)-protected benzyl amine moiety was synthesized at first (**2**, Scheme S1a and Figure S2). Heating of **2** leads to clean and quantitative transformation into isocyanate derivative,^[16] which *in situ* react with high quality mPEG₄₅-OH (Figure S1i) under DBTL catalysis to afford mPEG₄₅- $B-NH-Cbz$ (Scheme S1a). Upon hydrogenation, as-synthesized mPEG₄₅- $B-NH_2$ in the native unprotonated state could serve as a model compound to interrogate the effects of amine basicity and spacer linker on PEG-amine storage stabilities.

Both GPC and ¹H NMR confirmed quantitative transformation of mPEG₄₅-OH into mPEG₄₅- $B-NH-Cbz$ (Figures 1b and S3, Table S1). MALDI-TOF MS revealed high-fidelity terminal functionality by the presence of only one set of patterns corresponding to $[M+Na]^+$ (Figure S3b). Upon hydrogenation, GPC analysis of freshly synthesized mPEG- $B-NH_2$ revealed symmetric elution trace, with peak elution time intermediate between those of mPEG₄₅-OH and mPEG₄₅- $B-NH-Cbz$ precursors (Figure S1b). The symmetric GPC elution trace of mPEG- $B-NH_2$ is quite amazing as PEG-specialized manufacturers tend to interpret multimodal GPC traces of mPEG- NH_2 (Figure S1) to nonspecific interactions between terminal amine and GPC column packing materials. These results confirm that multimodal GPC traces are correlated with uncontrolled quality during both manufacturing

and storage period afterwards. Two sets of MS peaks are present on the MALDI-TOF MS of mPEG- $B-NH_2$, which are assigned $[M+Na]^+$ and $[M+Na+184.1]^+$ (Figures 1c and S4b). Note that the latter main MS peak is due to *in situ* addition reaction of terminal amine with DCTB matrix during MALDI sample preparation, as revealed by Meijer and coworkers.^[19] We further examined storage stability of as-prepared mPEG- $B-NH_2$. Upon storage at -20°C inside a glovebox for 7 d and accelerated aging at 60°C under vacuum for 7 d, respectively, we could observe the evolution of a slight shoulder peak at the high MW side and tailing at the low MW side; note that the total content of newly formed species is <5% (Figure S5). On the other hand, MALDI-TOF MS analysis revealed almost no changes, suggesting the complementarity between GPC and MALDI-TOF MS techniques. Upon storage in a glovebox at -20°C for ~ 1 year, GPC analysis revealed prominent broadening and emergence of at least two new peaks at higher MW side, implying interchain coupling and degradation reactions. Notably, MALDI-TOF MS analysis also revealed the shift to higher MW side, although MS peak assignments remained unchanged (Figure S5). These results suggested that in addition to flawed manufacturing protocols, storage stability issue of conventional mPEG- NH_2 originating from amine basicity remains a serious concern. mPEG- $B-NH_2$ could partially solve the stability issue due to decreased basicity of terminal benzyl amine and *N*-phenylcarbamate spacer. If applicable, storage of PEG-amine in the primary ammonium form provides to be a better alternative (refer to Figure S6 for the storage stability of mPEG₄₅- $B-NH_3^+Cl$).

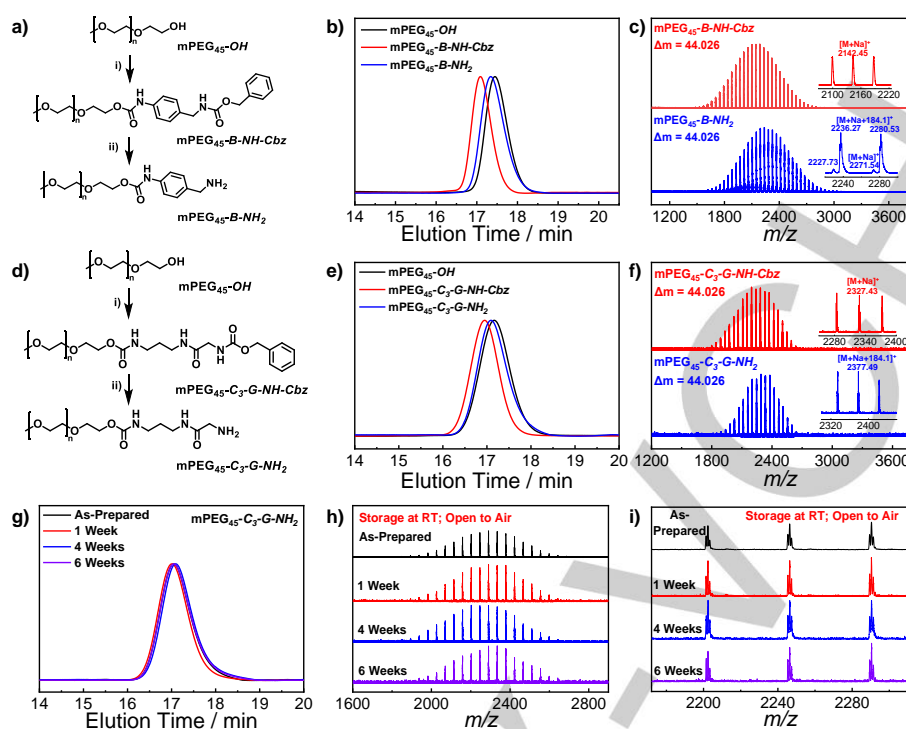


Figure 1. Schematics of the preparation of a) $m\text{PEG}_{45}\text{-B-NH}_2$ and d) $m\text{PEG}_{45}\text{-C}_3\text{-G-NH}_2$. b) GPC traces recorded in THF for $m\text{PEG}_{45}\text{-B-NH-Cbz}$ and $m\text{PEG}_{45}\text{-B-NH}_2$. c) MALDI-TOF mass spectra of $m\text{PEG}_{45}\text{-B-NH-Cbz}$ and $m\text{PEG}_{45}\text{-B-NH}_2$. e) GPC traces recorded in DMF for $m\text{PEG}_{45}\text{-C}_3\text{-G-NH-Cbz}$ and $m\text{PEG}_{45}\text{-C}_3\text{-G-NH}_2$. f) MALDI-TOF mass spectra of $m\text{PEG}_{45}\text{-C}_3\text{-G-NH-Cbz}$ and $m\text{PEG}_{45}\text{-C}_3\text{-G-NH}_2$. The storage stability of $m\text{PEG}_{45}\text{-C}_3\text{-G-NH}_2$ when exposed to air at room temperature, as assayed by g) GPC and h-i) MALDI-TOF MS characterization. For comparison, the GPC trace of $m\text{PEG}_{45}\text{-OH}$ is also shown in b) and e).

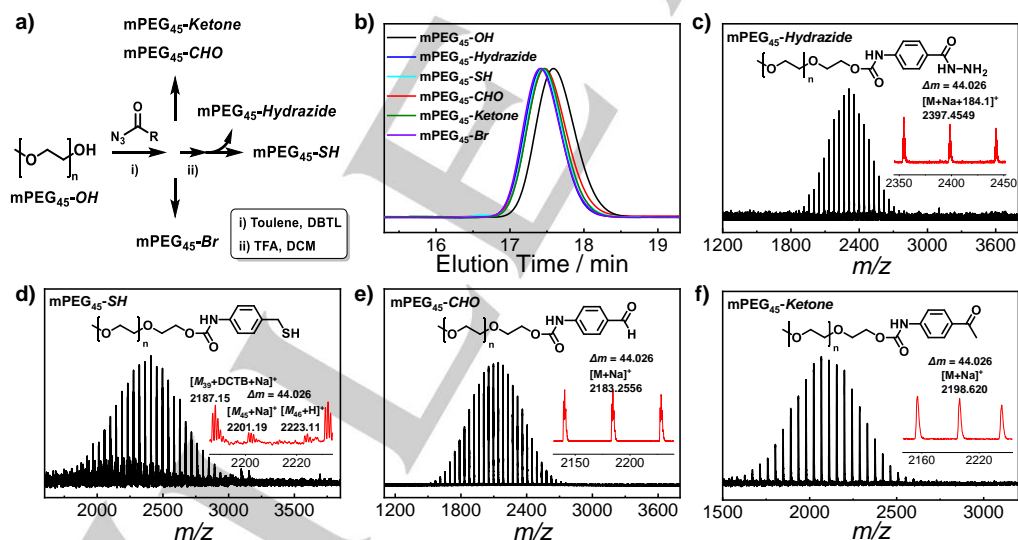


Figure 2. a) Synthetic routes and b) relevant GPC traces recorded in THF for $m\text{PEG}_{45}\text{-Hydrazide}$, $m\text{PEG}_{45}\text{-SH}$, $m\text{PEG}_{45}\text{-CHO}$, $m\text{PEG}_{45}\text{-Ketone}$, and $m\text{PEG}_{45}\text{-Br}$. MALDI-TOF mass spectra recorded for c) $m\text{PEG}_{45}\text{-Hydrazide}$, d) $m\text{PEG}_{45}\text{-SH}$, e) $m\text{PEG}_{45}\text{-CHO}$, and f) $m\text{PEG}_{45}\text{-Ketone}$.

We envisage that further decreasing terminal amine basicity could help enhance or even solve the stability issue of PEG-amine (Scheme 1b). *N*-Terminal amine of peptides typically possess lower much lower pK_a compared to ethylamine or benzyl amine moieties. Moreover, decreased basicity could also elevate the efficacy of amine-relevant conjugation reactions under neutral or even mildly acidic conditions.^[5b] $m\text{PEG}_{23}\text{-G-NH-Cbz}$ was facilely synthesized in one-pot via reaction of $m\text{PEG}_{23}\text{-OH}$ with *in situ* generated isocyanate derivative from acyl azide-containing precursor **3** upon heating (Scheme S1b, Figures S7-S8, Table S1).

However, the postulated hydrogenation product, $m\text{PEG}_{23}\text{-G-NH}_2$, is unstable and accompanied with spontaneous deamination and rearrangement (Scheme S1b). The undesired formation of PEG derivative with carbamate terminal was confirmed by GPC, NMR, and MALDI-TOF MS characterization (Figures S7-S8), and further corroborated by studies on small molecule model compounds (Scheme S1c and Figure S9).

We further attempted to incorporate spacer linker by starting with *Cbz-GG-acyl azide* (**8**, Scheme S2a). Unfortunately, upon hydrogenation, $m\text{PEG}_{45}\text{-C}_1\text{-G-NH}_2$ exhibits spontaneous amine-

mediated cyclization side reactions, although GPC elution traces remained monomodal and symmetric upon long-term storage under open air (Figures S10-S11). Considering that further extending the spacer length could inhibit cyclization and eliminate deamination reactions, mPEG₄₅-C₃-G-NH₂-Cbz with C₃ spacer was synthesized using **10** as the isocyanate precursor (Scheme S2b; Figure 1d; Figures S12-S13). Upon hydrogenation, high-fidelity fabrication of mPEG₄₅-C₃-G-NH₂ was accomplished, as revealed by the monomodal and symmetric GPC elution trace (Figure 1e) and the clean set of MALDI-TOF MS pattern (Figures 1f and S13). Furthermore, when exposed under open air for 1-6 weeks, both GPC and MALDI-TOF MS characterization revealed essentially no changes (Figure 1g-i), which is in stark contrast to commercial mPEG₄₅-NH₂ (Figure S1) and mPEG-B-NH₂ (Figure S5). These results indicate that the PEG-amine stability issue could be solved by finely tuning amine basicity/nucleophilicity (Scheme 1). The excellent storage stability of mPEG₄₅-C₃-G-NH₂ towards air oxidation and spontaneous chain degradation augurs well for its commercial manufacturing and storage. Under certain application circumstances, PEG-amine in the native form has to be used (e.g., amphiphilic PEG-polypeptide synthesis via NCA polymerization), as *in situ* deprotonation with organic bases will lead to alternate polymerization mechanisms.^[6c,20]

Building on the successful synthesis of high-fidelity and air-stable PEG-amine derivatives, we further explored the utilization of carbamate linkage to fabricate PEG-derivatives with a diverse range of terminal functionalities including hydrazide, thiol, aldehyde, ketone, maleimide, and bromine (Scheme 1). Note that these reactive groups are important for protein PEGylation and fabrication of drug conjugates.^[2] Due to functional compatibility between aldehyde/ketone and isocyanates, high-fidelity mPEG₄₅-CHO and mPEG₄₅-Ketone were facilely synthesized in one-step by directly reacting mPEG₄₅-OH with 4-formylbenzoyl azide (**16a**), and 4-acetylbenzoyl azide (**16b**), respectively (Figure 2b,e,f and Figures S20-S23). For the synthesis of PEG₄₅-Hydrazide and PEG₄₅-SH, a three-step approach was employed: i) synthesis of acyl azide derivative bearing Boc-protected benzoyl hydrazide (**13**) and Trt-protected benzyl mercaptan (**15**); ii) *in situ* reaction of **13** and **15** with mPEG₄₅-OH upon heating under DBTL catalysis; iii) deprotection by TFA treatment (Schemes S2-S3; Figure 2b-2d). All intermediates and products were thoroughly characterized by GPC, MALDI-TOF MS, and ¹H NMR, revealing quantitative transformation of mPEG₄₅-OH into corresponding end-functionalized mPEG₄₅ and high-fidelity terminal functionality (Figure 2, Figures S16-S23; Table S1). It is worthy of noting that MALDI-TOF MS patterns of PEG₄₅-Hydrazide and PEG₄₅-SH are very clean, with all MS peaks assignable to specified chemical structures (Figure 2c,d). Therefore, the "carbamate" strategy provides a facile and universal strategy for end-functionalized PEG with diverse reactive groups. In principle, it could be further generalized to the functionalization of any small molecules and polymer precursors bearing hydroxyl and amine moieties.

Maleimide functionality is also of vital importance towards the synthesis of functional bioconjugates.^[3] On the other hand, α,ω -bifunctional and 3-arm PEG have been extensively utilized for hydrogel and network fabrication.^[12c] We then utilized the "carbamate" strategy to synthesize high-fidelity multifunctional PEG derivatives bearing one, two, and three maleimide moieties. Considering the highly reactive nature of maleimide, acyl azide derivative containing furan-protected maleimide moiety, **20**, was prepared at first, followed by *in situ* reactions with mPEG₄₅-OH, PEG₄₅ diol, and 3-arm PEG₂₁-3OH upon heating to 85 °C, affording corresponding functionalized PEG with furan-protected

maleimide functionality. Next, mPEG₄₅-Mal, PEG₄₅-2Mal, and 3-arm PEG₂₁-3Mal were obtained by deprotection at 110 °C (Schemes 1 and S4). Again, ¹H NMR, GPC, and MALDI-TOF MS analysis indicated high-efficiency conversion and high-fidelity terminal functionality (Figure 3, Figures S24-S28). Notably, furan-protected maleimide moieties are unstable under the MALDI-TOF MS conditions and main MS peaks are assigned to [M+Na-Fu]⁺ (Figure S25b). The MALDI-TOF mass spectra of mPEG₄₅-Mal, PEG₄₅-2Mal, and 3-arm PEG₂₁-3Mal are extremely clean, exhibiting no discernible impurity peaks. These results confirmed high-fidelity functionalization and the feasibility of fabricating PEG derivatives with nonlinear chain topologies (Figure 3d,e,f; Figures S26-S28).

Based on the facile fabrication of PEG derivatives with carbamate linkage and incubation stability towards enzymatic hydrolysis,^[2c,13] we are curious about the effects of carbamate linkage on BCP self-assembly and relevant biomedical functions. Previously, mPEG-based ATRP and RAFT macroinitiators with ester bonds have been exclusively utilized to synthesize amphiphilic BCPs.^[4] We envisage that the use of alternate carbamate junction linkage could endow enhanced nanostructure stability in aqueous media and a new approach to PEGylated nanomaterials. We then synthesized a new PEG-based ATRP macroinitiator bearing carbamate linkage (mPEG₄₅-Carbamate-Br) through *in situ* reaction of 4-(bromomethyl)benzoyl azide (**21**) with mPEG₄₅-OH (Figure S29). For comparison, conventional ester-based mPEG₄₅-Ester-Br macroinitiator was also synthesized. Subsequent ATRP of styrene (St) using these two types of macroinitiators afforded PEG₄₅-Carbamate-PS_m and mPEG₄₅-Ester-PS_n with varying polystyrene (PS) block lengths (Scheme S5, Figures S30-S32; Table S2). Quite unexpectedly, both mPEG₄₅-Carbamate-PS₁₀₁ and mPEG₄₅-Carbamate-PS₄₆ self-assembled into vesicular nanostructures, whereas mPEG₄₅-Ester-PS₁₀₃ and mPEG₄₅-Ester-PS₄₃ with comparable hydrophobic PS lengths only self-assembled into micellar nanoparticles (Figure 4b-f and Figure S33). Previously, we reported that amphiphilic BCPs with the hydrophobic block bearing side chain or main chain carbamate moieties could promote self-assembly into higher-order nanostructures other than nanospheres.^[4f,4g,11a,21] In the current study, we discovered that the replacement of the single ester linkage into carbamate one at the diblock junction position could render a huge difference in self-assembling behaviors. We ascribe this phenomenon to interchain carbamate-mediated hydrogen bonding interactions at the core-shell interface (Scheme 1c, Figures 4b and S34), which facilitate morphological transition from spherical micelles into vesicles and provide additional stabilization of corresponding nanostructures. Note that carbamate-relevant hydrogen bonding interactions at the core-shell interface were further verified by temperature-dependent FT-IR for the corresponding micellar dispersion in D₂O, and this feature was completely absent for the counterpart BCP with ester linkage at the block junction (Figure S34).

Considering the use of self-assembled nanostructures as drug nanocarriers, we further evaluated the stability of self-assembled nanostructures against esterase, which is abundant in biological fluids such as blood serum.^[22] For direct comparison and clarity of GPC data interpretation, spherical micelles self-assembled from mPEG₄₅-Carbamate-PS₆ and mPEG₄₅-Ester-PS₆ BCPs were examined. Upon incubating the micellar dispersion with esterase for 0-120 h, esterase-mediated degradation of mPEG₄₅-Ester-PS₆ amphiphiles were clearly apparent, as evidenced from time-dependent GPC elution traces (Figure 4g). In sharp contrast,

COMMUNICATION

WILEY-VCH

micellar nanoparticles assembled from mPEG₄₅-Carbamate-PS₆ are resistant to both esterase hydrolysis and spontaneous hydrolysis under otherwise identical conditions (inset in Figure 4g), verifying the microstructural stability of carbamate linkages over ester bonds.^[2c,13]

Using clinically applied indocyanine green (ICG) as a model functional agent, it was found that mPEG₄₅-Carbamate-PS₆ micelles could efficiently load ICG with an encapsulation efficiency (EE) up to ~90% and loading content (LC) ~8.1%, in contrast to ~60% and ~5.7% for micelles of the ester counterpart, mPEG₄₅-Ester-PS₆ (Figure 4h). Due to improved stability against esterase, ICG release from mPEG₄₅-Carbamate-PS₆ micelles was remarkably prohibited, and less than ~10% ICG was released within 72 h incubation duration. On the other hand, >90% ICG was released from mPEG₄₅-Ester-PS₆ micelles. Under *in vivo* conditions, fluorescence emission of ICG-loaded mPEG₄₅-Carbamate-PS₆ micelles could still be detected 48 h after

intravenous injection into mice. For mPEG₄₅-Ester-PS₆ micelles, ICG emission completely diminished after 24 h under identical ICG injection levels (Figure 4j,k). These results demonstrated that the carbamate linkage provides extra advantages compared to conventional BCPs with ester junction linkage, synthesized via typical controlled radical polymerizations, due to cooperative hydrogen bonding interactions at the core-shell interface (Figures 4b and Figure S34). Overall, polymeric amphiphiles with carbamate moieties, located either in side linkages or at block junction point, could lead to robust self-assembled nanostructures with high drug loading capacity, enhanced encapsulation stability, and extended blood circulation lifetimes.^[4f,4g,11a,21a-e] In addition, the replacement of single ester junction linkage in amphiphilic BCPs with carbamate moiety, and its effects on both self-assembled nanoassemblies and relevant drug delivery functions are also reminiscent of “single point mutation” in the field of genetics and epigenetics.

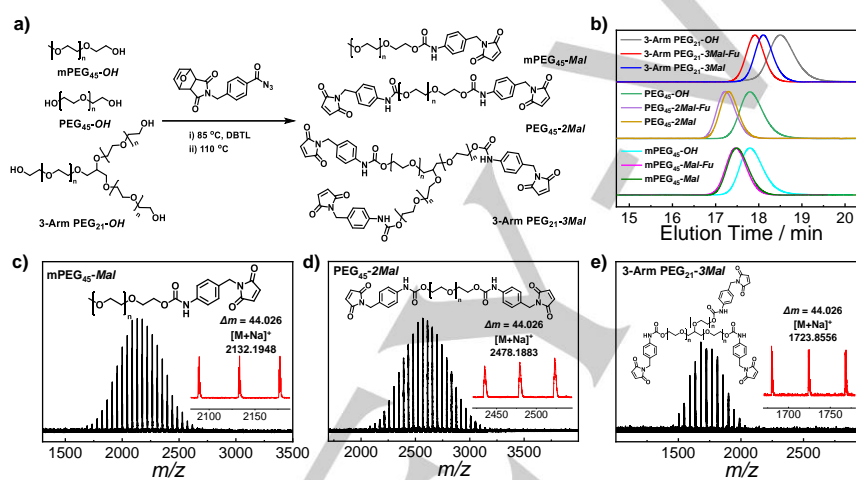


Figure 3. a) Synthetic routes and b) GPC traces recorded in THF for mPEG₄₅-Mal, PEG₄₅-2Mal, and 3-arm PEG₂₁-3Mal; GPC traces of PEG precursors and relevant intermediates are also shown for comparison. MALDI-TOF mass spectra recorded for c) mPEG₄₅-Mal, d) PEG₄₅-2Mal, and e) 3-arm PEG₂₁-3Mal.

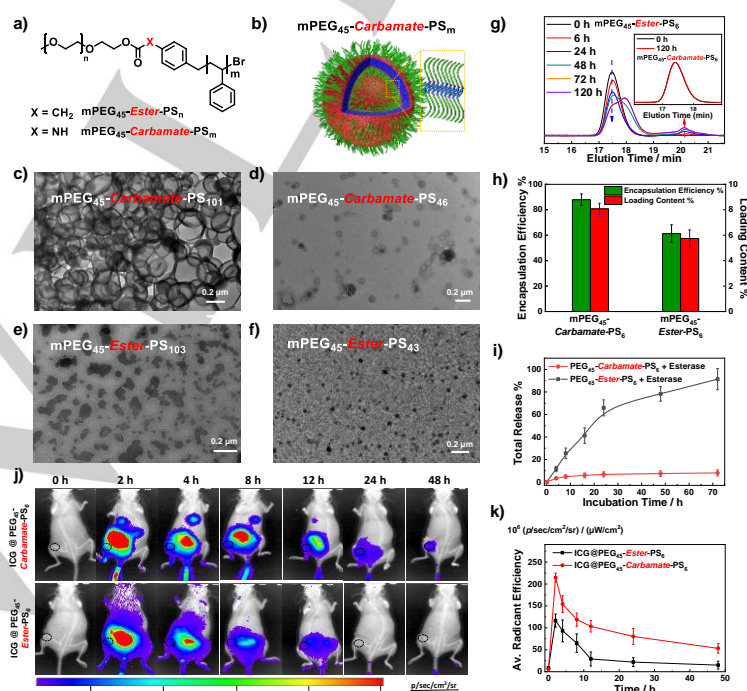


Figure 4. a) Chemical structures of amphiphilic BCPs with different junction linkages: mPEG₄₅-Ester-PS_n versus mPEG₄₅-Carbamate-PS_m. b) Schematics of vesicle formation from mPEG₄₅-Carbamate-PS_m and nanostructure stabilization facilitated by interchain hydrogen bonding interactions of carbamate linkages at diblock junctions; note that mPEG₄₅-Ester-PS_n with comparable PS lengths only self-assembles into micellar nanoparticles. Typical TEM images recorded for c) mPEG₄₅-Carbamate-PS₁₀₁, d) mPEG₄₅-Carbamate-PS₄₆, e) mPEG₄₅-Ester-PS₁₀₃, and f) mPEG₄₅-Ester-PS₄₃ nanoassemblies. g) Evolution of GPC traces recorded for mPEG₄₅-Ester-PS₆ and mPEG₄₅-Carbamate-PS₆ micelles upon incubation with esterase in PB buffer (pH 7.4, 10 mM). h) Comparison of loading efficiencies and loading contents of ICG by mPEG₄₅-Carbamate-PS₆ and mPEG₄₅-Ester-PS₆ micelles. i) Cumulative release profiles of ICG-loaded mPEG₄₅-Ester-PS₆ micelles and mPEG₄₅-Carbamate-PS₆ micelles upon incubation with esterase in PB buffer (pH 7.4, 10 mM). j) *In vivo* NIR fluorescence tumor imaging and k) evolution of average emission intensities at the tumor region for 4T1 tumor-bearing Balb/c mice at 2, 4, 8, 12, 24, and 48 h after intravenous injection of ICG-loaded mPEG₄₅-Ester-PS₆ micelles and mPEG₄₅-Carbamate-PS₆ micelles at an equivalent ICG dosage of 80 µg/kg.

In summary, we developed a highly efficient strategy to synthesize PEG derivatives with varying terminal with high-fidelity terminal functionalities including primary amine, hydrazide, thiol, aldehyde, ketone, maleimide, and bromide. The functionalization process is conducted in a one-pot manner by taking advantage of acyl azide chemistry, which quantitatively transforms *in situ* into isocyanate derivatives upon heating. The high-fidelity of PEG functionalization is verified by the clean set of MALDI-TOF MS patterns and monomodal/symmetric GPC elution traces. Storage-stable and air-insensitive PEG-amine was fabricated for the first time by integrating the “carbamate” strategy with finely tuned terminal amine basicity/nucleophilicity, together with appropriate choice of spacer linkers. Besides linear PEG, non-linear ones (e.g., star-shaped) could also be quantitatively functionalized without compromising conjugation efficiency. Notably, the incorporation of carbamate linkage instead of conventional ester bond at the diblock junction could not only facilitate higher-order nanostructure formation, but also remarkably improve nanostructure (encapsulation) stability under *in vitro* and *in vivo* conditions. In principle, the reported “carbamate” strategy could be further generalized to the functionalization of any small molecules and polymer precursors bearing hydroxyl and amine moieties.

Acknowledgements

The financial support from National Natural Science Foundation of China (NNSFC) Project (51690150, 51690154, 21674103, and U19A2094) and International S&T Cooperation Program of China (ISTCP) of MOST (2016YFE0129700) is gratefully acknowledged.

Conflict of interest

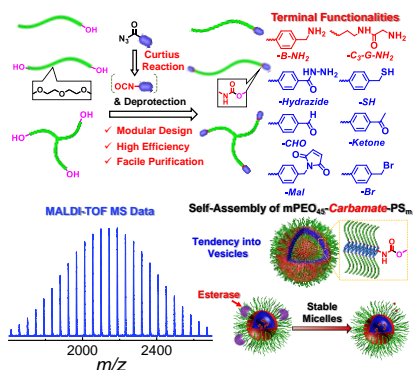
S.Y.L. and S.Y.S are inventors on a patent application filed by University of Science and Technology of China that covers end-group functionalization of hydroxyl-relevant compounds.

Keywords: functionalized PEG • carbamate linker • amphiphilic block copolymers • self-assembly • encapsulation stability

- [1] a) S. Zalipsky, *Adv. Drug Del. Rev.* **1995**, *16*, 157-182; b) J. M. Harris, S. Zalipsky, *Poly(ethylene glycol): Chemistry and Biological Applications*, ACS, Washington, DC, **1997**.
- [2] a) A. Abuchowski, J. R. McCoy, N. C. Palczuk, T. Van Es, F. F. Davis, *J. Biol. Chem.* **1977**, *252*, 3582-3586; b) R. Haag, F. Kratz, *Angew. Chem. Int. Ed.* **2006**, *45*, 1198-1215; *Angew. Chem.* **2006**, *118*, 1218-1237; c) R. B. Greenwald, Y. H. Choe, J. McGuire, C. D. Conover, *Adv. Drug Del. Rev.* **2003**, *55*, 217-250; d) G. Liu, G. Shi, H. Sheng, Y. Jiang, H. Liang, S. Liu, *Angew. Chem. Int. Ed.* **2017**, *56*, 8686-8691; *Angew. Chem.* **2017**, *129*, 8812-8817.
- [3] S. N. S. Alconcel, A. S. Baas, H. D. Maynard, *Polym. Chem.* **2011**, *2*, 1442-1448.
- [4] a) H. Otsuka, Y. Nagasaki, K. Kataoka, *Adv. Drug Del. Rev.* **2003**, *55*, 403-419; b) J. W. Singer, *J. Controlled Release* **2005**, *109*, 120-126; c) K. Osada, K. Kataoka, *Adv. Polym. Sci.* **2006**, *202*, 113-153; d) K. Knop, R. Hoogenboom, D. Fischer, U. S. Schubert, *Angew. Chem. Int. Ed.* **2010**, *49*, 6288-6308; *Angew. Chem.* **2010**, *122*, 6430-6452; e) Z. S. Ge, S. Y. Liu, *Chem. Soc. Rev.* **2013**, *42*, 7289-7325; f) Y. Li, G. Liu, X. Wang, J. Hu, S. Liu, *Angew. Chem. Int. Ed.* **2016**, *55*, 1760-1764; *Angew. Chem.* **2016**, *128*, 1792-1796; g) Z. Deng, Y. Qian, Y. Yu, G. Liu, J. Hu, G. Zhang, S. Liu, *J. Am. Chem. Soc.* **2016**, *138*, 10452-10466.
- [5] a) A. F. Bückmann, M. Morr, G. Johansson, *Makromol. Chem.* **1981**, *182*, 1379-1384; b) S. Zalipsky, *Bioconjugate Chem.* **1995**, *6*, 150-165; c) M. Leonard, E. Dellacherie, *Makromol. Chem.* **1988**, *189*, 1809-1817; d) J. M. Harris, *J. Macromol. Sci.: Part C* **1985**, *25*, 325-373.
- [6] a) T. J. Deming, *Chem. Rev.* **2016**, *116*, 786-808; b) N. Hadjichristidis, H. Iatrou, M. Pitsikalis, G. Sakellariou, *Chem. Rev.* **2009**, *109*, 5528-5578; c) Z. Y. Song, Z. Y. Han, S. X. Lv, C. Y. Chen, L. Chen, L. C. Yin, J. J. Cheng, *Chem. Soc. Rev.* **2017**, *46*, 6570-6599.
- [7] P.-C. Chen, Y. Liu, J. S. Du, B. Meckes, V. P. Dravid, C. A. Mirkin, *J. Am. Chem. Soc.* **2020**, *142*, 7350-7355.
- [8] a) J. Locquifier, J. Crommen, J. Vandorpe, E. Schacht, *Makromol. Chem. Rapid Commun.* **1991**, *12*, 159-165; b) D. L. Elbert, J. A. Hubbell, *Biomacromolecules* **2001**, *2*, 430-441; c) A. Karatzas, J. S. Haataja, D. Skoulas, P. Bilalis, S. Varlas, P. Apostolidi, S. Sofianopoulou, E. Stratikos, N. Houbenov, O. Ikkala, H. Iatrou, *Biomacromolecules* **2019**, *20*, 4546-4562; d) N. J. Warren, O. O. Mykhaylyk, D. Mahmood, A. J. Ryan, S. P. Armes, *J. Am. Chem. Soc.* **2014**, *136*, 1023-1033.
- [9] B. Banasik, C. Nadala, M. Samadpour, *Org. Prep. Proced. Int.* **2018**, *50*, 95-99.
- [10] a) S. Zalipsky, C. Gilon, A. Zilkha, *J. Macromol. Sci.: Part A* **2006**, *21*, 839-845; b) Y. Wei, R. Zhuo, X. Jiang, *J. Sep. Sci.* **2016**, *39*, 4305-4313.
- [11] a) X. Wang, G. Liu, J. Hu, G. Zhang, S. Liu, *Angew. Chem. Int. Ed.* **2014**, *53*, 3138-3142; *Angew. Chem.* **2014**, *126*, 3202-3206; b) F. Z. Lu, X. Y. Xiong, Z. C. Li, F. S. Du, B. Y. Zhang, F. M. Li, *Bioconjugate Chem.* **2002**, *13*, 1159-1162; c) G. Liu, C. M. Dong, *Biomacromolecules* **2012**, *13*, 1573-1583.
- [12] a) K. Maranski, Y. G. Andreev, P. G. Bruce, *Angew. Chem. Int. Ed.* **2014**, *53*, 6411-6413; *Angew. Chem.* **2014**, *126*, 6529-6531; b) N. Boden, R. J. Bushby, S. Clarkson, S. D. Evans, P. F. Knowles, A. Marsh, *Tetrahedron* **1997**, *53*, 10939-10952; c) Y. Z. Wei, R. X. Zhuo, X. L. Jiang, *J. Chromatogr.* **2016**, *1447*, 122-128.
- [13] a) C. Y. Cho, E. J. Moran, S. R. Cherry, J. C. Stephans, S. P. A. Fodor, C. L. Adams, A. Sundaram, J. W. Jacobs, P. G. Schultz, *Science* **1993**, *261*, 1303-1305; b) M. Shamis, H. N. Lode, D. Shabat, *J. Am. Chem. Soc.* **2004**, *126*, 1726-1731; c) X. Hu, S. Liu, Y. Huang, X. Chen, X. Jing, *Biomacromolecules* **2010**, *11*, 2094-2102; d) D. Aydin, M. Arslan, A. Sanyal, R. Sanyal, *Bioconjugate Chem.* **2017**, *28*, 1443-1451.
- [14] “End-group functionalization of hydroxyl-relevant compounds and polymers and methods therefor”: S. Y. Liu, S. Y. Shi, Patent Application Filed, CN202010578627.0, **2020**.
- [15] a) J. Glastrup, *Polym. Degrad. Stab.* **1996**, *52*, 217-222; b) A. Sayari, A. Heydari-Gorji, Y. Yang, *J. Am. Chem. Soc.* **2012**, *134*, 13834-13842.
- [16] P. Bollini, S. Choi, J. H. Drese, C. W. Jones, *Energy Fuels* **2011**, *25*, 2416-2425.
- [17] C. Godoy-Alcántar, A. K. Yatsimirsky, J. M. Lehn, *J. Phys. Org. Chem.* **2005**, *18*, 979-985.
- [18] M. V. Zabalov, R. P. Tiger, *Russ. Chem. Bull.* **2007**, *56*, 7-13.
- [19] X. Lou, B. F. de Waal, J. L. van Dongen, J. A. Vekemans, E. W. Meijer, *J. Mass Spectrom.* **2010**, *45*, 1195-1202.
- [20] H. R. Kricheldorf, *Angew. Chem. Int. Ed.* **2006**, *45*, 5752-5784; *Angew. Chem.* **2006**, *118*, 5884-5917.
- [21] a) G. Liu, X. Wang, J. Hu, G. Zhang, S. Liu, *J. Am. Chem. Soc.* **2014**, *136*, 7492-7497; b) X. Wang, J. Hu, G. Liu, J. Tian, H. Wang, M. Gong, S. Liu, *J. Am. Chem. Soc.* **2015**, *137*, 15262-15275; c) X. R. Wang, C. Z. Yao, G. Y. Zhang, S. Y. Liu, *Nature Commun.* **2020**, *11*, 13; d) C. Z. Yao, X. R. Wang, J. M. Hu, S. Y. Liu, *Acta Polym. Sin.* **2019**, *50*, 553-566; e) J. M. Hu, S. Y. Liu, *Sci. China Chem.* **2018**, *61*, 1110-1122; f) Z. Y. Deng, S. Yuan, R. X. Xu, H. J. Liang, S. Y. Liu, *Angew. Chem. Int. Ed.* **2018**, *57*, 8896-8900; *Angew. Chem.* **2018**, *130*, 9034-9038.
- [22] a) F. Liu, Z. Zhao, J. Yang, J. Wei, S. Li, *Polym. Degrad. Stab.* **2009**, *94*, 227-233; b) R. J. Amir, S. Zhong, D. J. Pochan, C. J. Hawker, *J. Am. Chem. Soc.* **2009**, *131*, 13949-13951; c) X. Zhu, M. Fryd, B. D. Tran, M. A. Ilies, B. B. Wayland, *Macromolecules* **2012**, *45*, 660-665; d) J. Rosselgong, E. G. L. Williams, T. P. Le, F. Grusche, T. M. Hinton, M. Tizard, P. Gunatillake, S. H. Thang, *Macromolecules* **2013**, *46*, 9181-9188; e) N. Qiu, X. Liu, Y. Zhong, Z. Zhou, Y. Piao, L. Miao, Q. Zhang, J. Tang, L. Huang, Y. Shen, *Adv. Mater.* **2016**, *28*, 10613-10622; f) Y. Zheng, B. Yu, Z. Li, Z. Yuan, C. L. Organ, R. K. Trivedi, S. Wang, D. J. Lefer, B. Wang, *Angew. Chem. Int. Ed.* **2017**, *56*, 11749-11753; *Angew. Chem.* **2017**, *129*, 11911-11915; g) A. Tatsumi, S. Inoue, T. Hamaguchi, S. Iwakawa, *Biol. Pharm. Bull.* **2018**, *41*, 277-280; h) C. Yao, Y. Li, Z. Wang, C. Song, X. Hu, S. Liu, *ACS Nano* **2020**, *14*, 1919-1935.

Entry for the Table of Contents

COMMUNICATION



Storage-stable and air-insensitive PEG-amine with high-fidelity functionality was constructed via integrating carbamate linkage with finely tuned amine basicity. The "carbamate" strategy provides a general approach towards PEG derivatives with diverse functionalities. Carbamate linkage at diblock junction facilitates self-assembly into higher-order nanostructures with improved stability towards both hydrolysis and drug encapsulation.

S. Shi, C. Yao, J. Cen, L. Li, G. Liu, J. Hu, S. Liu*

Page No. – Page No.

High-Fidelity End-Functionalization of Poly(ethylene glycol) Using Stable and Potent Carbamate Linkages